


RESEARCH PAPER



## A stable tRNA-like molecule is generated from the long noncoding RNA *GUT15* in *Arabidopsis*

Patrycja Plewka<sup>a</sup>, Agnieszka Thompson <sup>b</sup>, Maciej Szymanski<sup>b</sup>, Przemyslaw Nuc<sup>a</sup>, Katarzyna Knop<sup>a</sup>, Agnieszka Rasinska<sup>b</sup>, Aleksandra Bialkowska<sup>a</sup>, Zofia Szweykowska-Kulinska<sup>a</sup>, Wojciech M. Karlowski<sup>b</sup> and Artur Jarmolowski<sup>a</sup>

<sup>a</sup>Department of Gene Expression, Faculty of Biology, Institute of Molecular Biology and Biotechnology, Adam Mickiewicz University in Poznan, Poznan, Poland; <sup>b</sup>Department of Computational Biology, Faculty of Biology, Institute of Molecular Biology and Biotechnology, Adam Mickiewicz University in Poznan, Poznan, Poland

### ABSTRACT

The *Arabidopsis GUT15* RNA belongs to a class of noncoding RNAs that are expressed from the intergenic regions of protein-coding genes. We show that the RNA polymerase II transcribed *GUT15* transcript serves as a precursor for two stable RNA species, a tRNA-like molecule and *GUT15*-tRF-F5, which are both encoded by the final intron in the *GUT15* gene. The *GUT15*-encoded tRNA-like molecule cannot be autonomously transcribed by RNA polymerase III. However, this molecule contains a CCA motif, suggesting that it may enter the tRNA maturation pathway. The *GUT15*-encoded tRNA-like sequence has an inhibiting effect on the splicing of its host intron. Moreover, we demonstrate that the canonical tRNA genes nested within introns do not affect the splicing patterns of their host protein-coding transcripts.

### ARTICLE HISTORY

Received 6 December 2017  
Accepted 21 February 2018

### KEYWORDS

*Arabidopsis*; lncRNAs; *GUT15*; tRNA-like; splicing



## Introduction

Recent advances in RNA sequencing technology and computational analyses have resulted in the identification of a notable number of long transcripts known as long noncoding RNAs (lncRNAs) that lack protein-coding capacity [1]. The heterogeneity in the biogenesis, expression levels, stability and evolution of this diverse class of molecules reflects the broad array of functions performed by lncRNAs in the cell. Based on animal studies, lncRNAs have emerged as novel factors regulating different aspects of gene expression, and these factors have been shown to participate in transcriptional silencing by recruiting chromatin remodeling complexes [2]. Several lines of evidence suggest that lncRNAs play a role in establishing and maintaining the architecture of nuclear compartments [2].

Numerous lncRNAs have been predicted and identified in several plant species [3]; however, our knowledge regarding their biogenesis and molecular functions remains limited to a few examples. Both *AtCOOLAIR* and *AtCOLDAIR* noncoding RNAs play roles in the epigenetic silencing of the *FLC* locus during vernalization [4,5]. The epigenetic landscape is also affected by the dual noncoding transcription of the *APOLO* locus (performed by both RNA polymerase II and V) that controls the auxin-driven chromatin loop dynamics to regulate the expression of the neighboring *PID* gene, which encodes an essential regulator of polar auxin transport [6]. The *APOLO* lncRNA-dependent oscillating chromatin topology further reflects an additional function ascribed to plant lncRNAs, i.e., the production of small interfering RNAs [7]. Generally, the

biogenesis of 24 nt siRNAs requires noncoding transcription, which is driven by plant RNA polymerases IV and V, and leads to transcriptional gene silencing (TGS) by directing the DNA methylation of their locus of origin and adjacent genes [8]. In addition, plant lncRNAs have been associated with other biological processes. Phosphate homeostasis is regulated by the *IPS1* lncRNA, which acts as an endogenous target mimic of miR399 [9]. Photomorphogenesis in *Arabidopsis* seedlings is regulated by the *HID3* lncRNA, which is known to associate with *PIF3* locus chromatin and repress its transcription [10]. In rice, the *LDMAR* noncoding transcript is required for normal male fertility under long-day conditions [11]. Plant lncRNAs are also involved in root nodule organogenesis; for example, the *ENOD40* lncRNA plays a role in the cytoplasmic re-location of the nuclear protein RBP1 during nodulation in *Medicago truncatula* [12]. Bardou and coworkers [13] identified that the *ASCO* lncRNA is a novel player (competitor) in the regulation of alternative splicing. Recently, the *ELENA1* noncoding transcript has been shown to be involved in the transcriptional regulation of plant innate immunity by interacting with Mediator and enhancing the expression of *PR1* (*PATHOGENESIS-RELATED 1*) [14].

Long noncoding RNAs can be classified into the following five different classes according to their genomic location: natural antisense transcripts (NATs), intronic noncoding RNAs, enhancer RNAs, promoter-associated transcripts and large intergenic noncoding RNAs (lincRNAs) [1]. The lincRNA group is represented in *A. thaliana* by the *GUT15* long

**CONTACT** Artur Jarmolowski  [artjarmo@amu.edu.pl](mailto:artjarmo@amu.edu.pl)  Department of Gene Expression, Faculty of Biology, Institute of Molecular Biology and Biotechnology, Adam Mickiewicz University in Poznan, Poznan, Poland.

 Supplementary data are available online at  <https://doi.org/10.1080/15476286.2018.1445404>.

© 2018 The Author(s). Published by Informa UK Limited, trading as Taylor & Francis Group

This is an Open Access article distributed under the terms of the Creative Commons Attribution-NonCommercial-NoDerivatives License (<http://creativecommons.org/licenses/by-nc-nd/4.0/>), which permits non-commercial re-use, distribution, and reproduction in any medium, provided the original work is properly cited, and is not altered, transformed, or built upon in any way.

noncoding transcript, which was first reported in tobacco as a short-lived RNA [15].

In this paper, we prove the existence of a tRNA-like structure nested within the gene encoding the *Arabidopsis* lncRNA *GUT15*. Interestingly, the biogenesis of this tRNA-like molecule relies on *GUT15* transcript processing rather than on RNA polymerase III-driven transcription. Furthermore, the CCA trinucleotide, which is indicative of functional tRNAs, is added to the 3'-end of the tRNA-like molecule encoded by the final intron of the *GUT15* primary transcript, and this molecule is most likely aminoacylated. Additionally, we show that the *GUT15*-encoded tRNA-like structure inhibits the splicing of its hosting intron.

## Results

### A tRNA-like molecule is encoded within the *Arabidopsis* lncRNA *GUT15* locus

The re-annotation of the tRNA genes in the *Arabidopsis* genome performed in our laboratory revealed the presence of a

tRNA-like sequence within the locus encoding the lncRNA *GUT15* (Gene with unstable transcript 15; At2g18440) [16]. This tRNA-like sequence exhibits the conserved structural features present in canonical tRNAs. In particular, the length of the acceptor, the D- and T-stems, as well as the size of the D- and T-loops are consistent with the standard tRNA structure cloverleaf model (Fig. 1A, left panel) [17]. Interestingly, compared with bona fide tRNA sequences, the sequence of the T-loop (positions 3–9 of the B-box in the sequence logo) in the identified tRNA-like structure is very well conserved. This feature plays a role in the formation of the distinct L-shaped tertiary structure that is essential for tRNA function. In contrast, the A-box of the *GUT15* tRNA-like structure differs from the consensus sequence due to two additional nucleotides (Fig. 1A, middle panel). Moreover, the region corresponding to the anticodon stem-loop in the tRNA-like structure cannot form the canonical 5-bp stem and 7-nucleotide loop. Another feature distinguishing the *GUT15* tRNA-like structure from standard tRNA molecules is the presence of three rather than two unpaired bases at the junction between the acceptor and

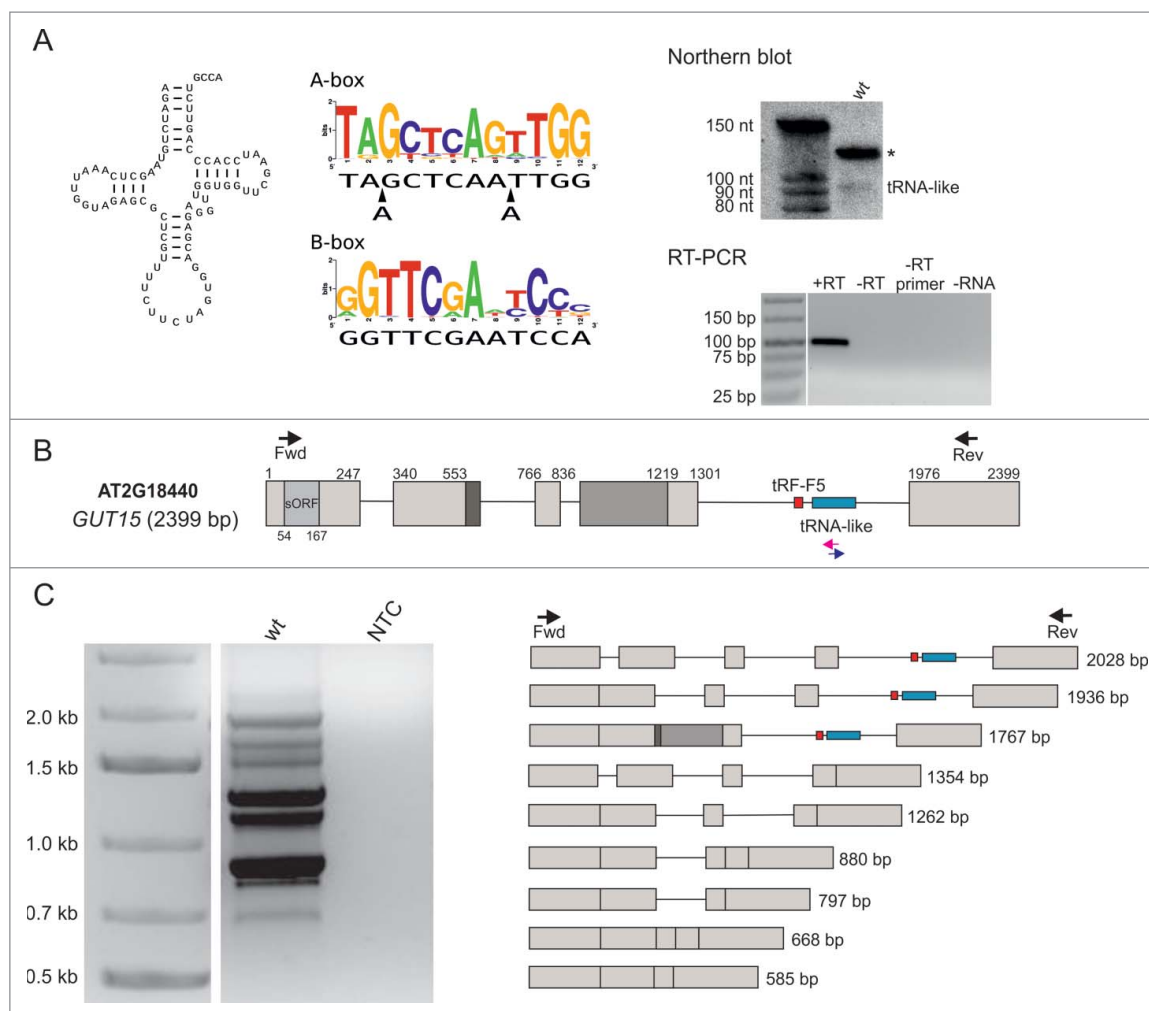


**Figure 1.** The *Arabidopsis* *GUT15* lncRNA contains a tRNA-like sequence in its final intron. (A) The *GUT15* tRNA-like secondary structure (left panel). Alignment of the *GUT15*-encoded tRNA-like molecule A-box and B-box to the consensus sequence profile of canonical tRNA promoter elements (middle panel). The tRNA-like sequence accumulation levels detected by Northern blotting and stem-loop RT-PCR in *Arabidopsis* seedlings (right panel). The asterisk corresponds to an unspecific band. +RT, the complete stem-loop RT-PCR reaction; -RT, no reverse transcriptase control; -RT primer, no stem-loop RT primer control; -RNA, no RNA control of the reverse transcription reaction. Marker in Northern, Decade™ Marker RNA (Thermo Fisher Scientific); marker in RT-PCR, Low Range DNA ladder (Thermo Fisher Scientific). (B) Structure of the *GUT15* gene hosting the tRNA-like sequence within its final intron. Boxes represent exons, lines depict introns, and arrows represent the primers used in the RACE (blue and pink) and RT-PCR analyses (black). (C) RT-PCR analysis showing different *GUT15* lncRNA splicing isoforms. Wt, cDNA template prepared from 10-day-old wild-type *Arabidopsis* seedlings; NTC, non-template control; marker, 1 kb plus (Thermo Fisher Scientific).

D-stem (Fig. 1A, left panel). The accumulation of the tRNA-like molecule encoded by *GUT15* in *Arabidopsis* seedlings was validated by RNA sequencing (unpublished) and confirmed by Northern blotting and stem-loop RT-PCR (Fig. 1A, right panel). Importantly, the *GUT15* tRNA-like molecule contains a CCA motif that is not encoded in the genome (Fig. 1A, left panel). Moreover, according to our tRNA-seq data, the tRNA-like RNA originating from *GUT15* was detected in the pool of deacylated tRNA molecules, suggesting that this RNA can be aminoacylated.

### The *GUT15* transcripts are capped, polyadenylated and undergo alternative splicing

To determine the structure of the transcripts originating from the *Arabidopsis GUT15* locus, we performed 5'- and 3'-RACE experiments using primers that hybridize to the tRNA-like sequence, followed by RT-PCR amplification of the products obtained with primers designed to bind to the 5'- and 3'-ends of the longest RACE fragments. Using this approach, we identified polyadenylated *GUT15* transcripts. Additionally, using the 5'-RLM-RACE procedure to selectively amplify only full-length capped RNAs, we showed that all analyzed *GUT15* transcripts contained the cap structure, which, along with the poly(A) tail, constitutes the characteristics of transcription driven by RNA polymerase II (RNAPII). Based on the longest 3'- and 5'-RACE products, we calculated the length of the *GUT15* lncRNA as 2399 bp (Fig. 1B). The presence of this full-length transcript was confirmed by RT-PCR. The experimentally established length of the *GUT15* lncRNA from *Arabidopsis* seedlings was 100 bp longer than the *GUT15* transcript described in the TAIR10 database [18]. However, this discrepancy may be due to differences in the regulation of *GUT15* gene transcription in specific tissues or the different developmental stages during which the RNA samples were collected. The *Arabidopsis GUT15* gene contains 4 introns. The discovered tRNA-like sequence is encoded by the final intron in the *GUT15* transcripts (Fig. 1B). Interestingly, the RT-PCR amplification of the *GUT15* cDNA revealed the presence of a series of splicing isoforms, and only three isoforms contained the tRNA-like-bearing intron (Fig. 1C).

### The *GUT15*-encoded tRNA-like sequence affects the splicing of its host intron

The mapping of the small RNA-seq data to the *GUT15* gene revealed a short sequence originating from the 5'-flanking region of the tRNA-like coding region in the final *GUT15* intron (Fig. 1B). We called this new small RNA molecule *GUT15*-tRF-F5 according to our previously proposed nomenclature [19]. The abundance of this molecule in different small RNA libraries is summarized in Table 1.

The close localization of the tRNA-like and *GUT15*-tRF-F5 sequences within the *GUT15* lncRNA intron raised the following two possible scenarios regarding the biogenesis of the tRNA-like molecule and *GUT15*-tRF-F5: 1) *GUT15*-tRF-F5 and the tRNA-like molecule are generated from a tRNA-like precursor that is transcribed by RNA polymerase III (RNAPIII) or 2) alternatively, the *GUT15*-tRF-F5 and tRNA-like sequences

**Table 1.** sRNA-seq results (homemade libraries and public samples) for *GUT15*-tRF-F5 AAAAGAGATCAAAGAG.

sample	count
cbc	251
cp1-3	140
serrate	226
hyl1-2	178
drb2	83
drb3	136
drb4	112
drb5	57
dcl2-5_14	164
dcl3-1_14	138
dcl4-2_14	203
rd6-15	85
sgs3-13	556
xrn2-3	605
xrn4-3	208
rdr2-2	353
rdr3b	126
rrp61-2	721
rrp62-1	224
rrp63-1	155
rns2-2	12
trz4	182
wt31	83
wt14	589
heat_c1	1
heat_c2	1
heat_c3	1
heat_30min_s1	1
heat_30min_s2	1
heat_6h_s3	1
drought_30pct_c3	1
cu_d_s1	1
cu_d_s2	1
cu_d_s3	1
nacl_e_s1	5
nacl_e_s3	1
sulfur_d_s1	1
cadmium_e_s1	1
cadmium_e_s2	4
SRR037653	20
SRR037656	6
SRR037657	17
SRR037658	13
SRR037659	6
SRR037660	26
SRR037663	18
SRR037664	27
SRR037665	20
SRR037666	8
SRR037667	24
SRR037669	17
SRR037670	4
SRR037675	24

are processed from *GUT15* transcripts or already spliced introns carrying both the tRNA-like molecule and *GUT15*-tRF-F5. To examine the relationship between the proximity of the tRNA-like structure and biogenesis of *GUT15*-tRF-F5, we created genetic constructs encoding the following two versions of the *GUT15* gene (both under the control of the CaMV 35S promoter): the full-length (35S-*GUT15*wt) version or a version lacking the tRNA-like sequence (35S-*GUT15*Δ); we introduced these constructs into *Nicotiana benthamiana* leaves using the agroinfiltration method (Fig. 2A). Using RT-PCR, we determined that the deletion of the tRNA-like sequence increases the splicing efficiency of its hosting intron (Fig. 2B). Moreover, the Northern blotting results showed an accumulation of processed *GUT15*-tRF-F5 from the mutated *GUT15* gene variant

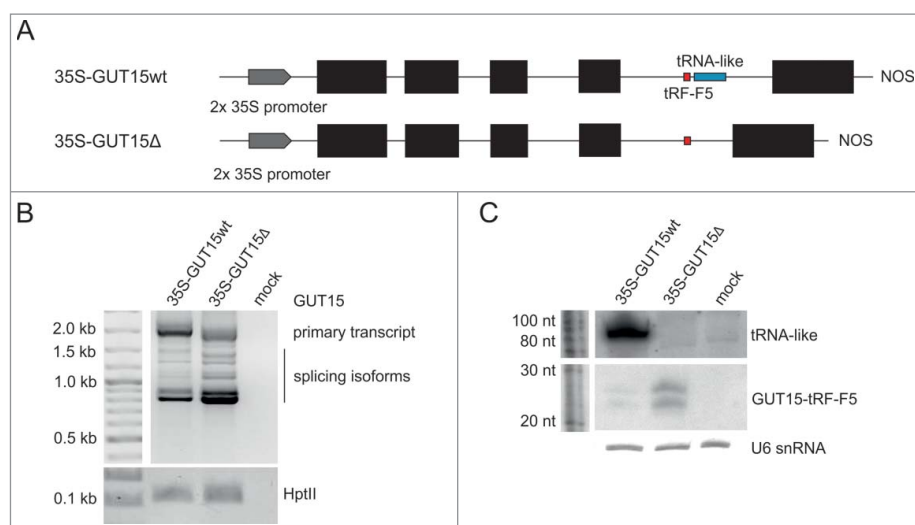


**Figure 2.** The tRNA-like sequence regulates the splicing of its host intron and the biogenesis of the *GUT15*-tRF-F5 small RNA. (A) Schematic representation of the *GUT15* gene variants used. Black boxes represent exons, and lines depict introns. Positions of the tRNA-like and *GUT15*-tRF-F5 sequences are marked in blue and red, respectively. NOS, transcription terminator. (B) Primary transcripts and splicing isoforms of *GUT15* detected by RT-PCR in *N. benthamiana* leaves infiltrated with the *GUT15* gene variants shown in A. The expression of the hygromycin phosphotransferase gene (*HptII*) served as a positive control for the agroinfiltration experiment. Marker, 100 bp plus (Thermo Fisher Scientific). MOCK is a negative control for the agroinfiltration experiments (leaves infiltrated only with MES buffer). (C) The accumulation levels of the tRNA-like and *GUT15*-tRF-F5 sequences detected by Northern blotting in infiltrated leaves expressing the *GUT15* gene variants shown in A. U6 snRNA serves as an RNA loading control. Marker, Decade™ Marker RNA (Thermo Fisher Scientific).

lacking the tRNA-like sequence, suggesting that the proximity of the tRNA-like molecule negatively affects the expression of *GUT15*-tRF-F5 (Fig. 2C, middle panel). Importantly, this result excluded the possibility that *GUT15*-tRF-F5 is produced from the tRNA-like precursor because the deletion of the tRNA-like molecule resulted in *GUT15*-tRF-F5 overexpression. Overall, the intronic *GUT15* tRNA-like sequence affects both the splicing of the final intron in the *GUT15* lncRNA and the accumulation of *GUT15*-tRF-F5.

#### The *GUT15*-encoded tRNA-like molecule is generated from the *GUT15* lncRNA

Thus far, we have shown that the tRNA-like sequence is transcribed as a part of the lncRNA *GUT15*, which is synthesized by RNAPII. However, this observation does not exclude that the tRNA-like locus can be independently transcribed also by RNAPIII. To address this issue, we transfected *N. tabacum* protoplasts with a *GUT15* native construct lacking any upstream regulatory sequences ( $\Delta$ p-GUT15wt) to investigate the activity of the internal A-box and B-box tRNA promoter elements within the *GUT15* tRNA-like sequence (Fig. 3A, upper panel, and Fig. 1A). The internal promoter elements within the tRNA-like coding sequence were not sufficient to drive its autonomous transcription by RNAPIII (Fig. 3B-C). In contrast, the *GUT15* tRNA-like molecule was detected in tobacco protoplasts transfected with the UBQ promoter-driven *GUT15* construct (Fig. 3B-C). Thus, the *GUT15*-encoded tRNA-like molecule can be processed from RNAPII-produced *GUT15* transcripts independently of the promoter used, i.e., the native or UBQ promoter. Moreover, no differences were observed in the tRNA-like sequence expression levels when the 35S-GUT15 $\Delta$ 5'3'ss construct with mutated 5'- and 3'- splice sites in the tRNA-like hosting intron was transiently expressed in the tobacco leaves (Fig. 3A, lower panel, and 3D-E). Thus, the biogenesis of the

tRNA-like molecule encoded within the *GUT15* intron is reliant on RNAPII *GUT15* transcription but independent of the *GUT15* final intron splicing.

#### Canonical tRNA genes nested within introns of protein-coding genes do not affect the splicing patterns of their host transcripts

Because the tRNA-like structure in the *GUT15*'s final intron affects its splicing, we globally examined the occurrence of tRNAs in genes across the *A. thaliana* genome. The computational analyses identified 19 protein-coding genes containing tRNA sequences in a sense context (in introns and untranslated regions (UTRs)) (Table 2). RT-PCR performed for 3 of these genes revealed that introns containing tRNAs are efficiently spliced in *Arabidopsis* seedlings (Fig. S3). Subsequently, we selected a gene encoding oligosaccharyltransferase (At3g12587) as an example to study the influence of tRNA sequences on the splicing of their host introns using a transient expression assay in *N. benthamiana* leaves (Fig. 4A-B). In contrast to the *GUT15* transcript, no notable differences were detected in the intron splicing efficiency when the naturally occurring tRNA-Arg<sup>CCG</sup> was removed from its host intron (Fig. 4C). Thus, the standard tRNA molecules embedded in the introns of protein-coding genes do not have a negative effect on the splicing of their host introns. To further validate this observation, we prepared the following two variants of the original *GUT15* intron 4 (pGUT15): in one variant, the tRNA-like sequence was removed (pGUT15 $\Delta$ ), and in the other variant, the *GUT15* tRNA-like sequence was replaced with the tRNA-Ala<sup>AGC</sup> gene (At1g06610; pGUT15(Ala)) (Fig. 5A-B, left panel). These constructs were introduced into *N. tabacum* protoplasts, and their intron excision efficiency was tested using RT-qPCR. All analyzed versions of the *GUT15* intron were efficiently spliced in the tobacco protoplast transient expression system. However,



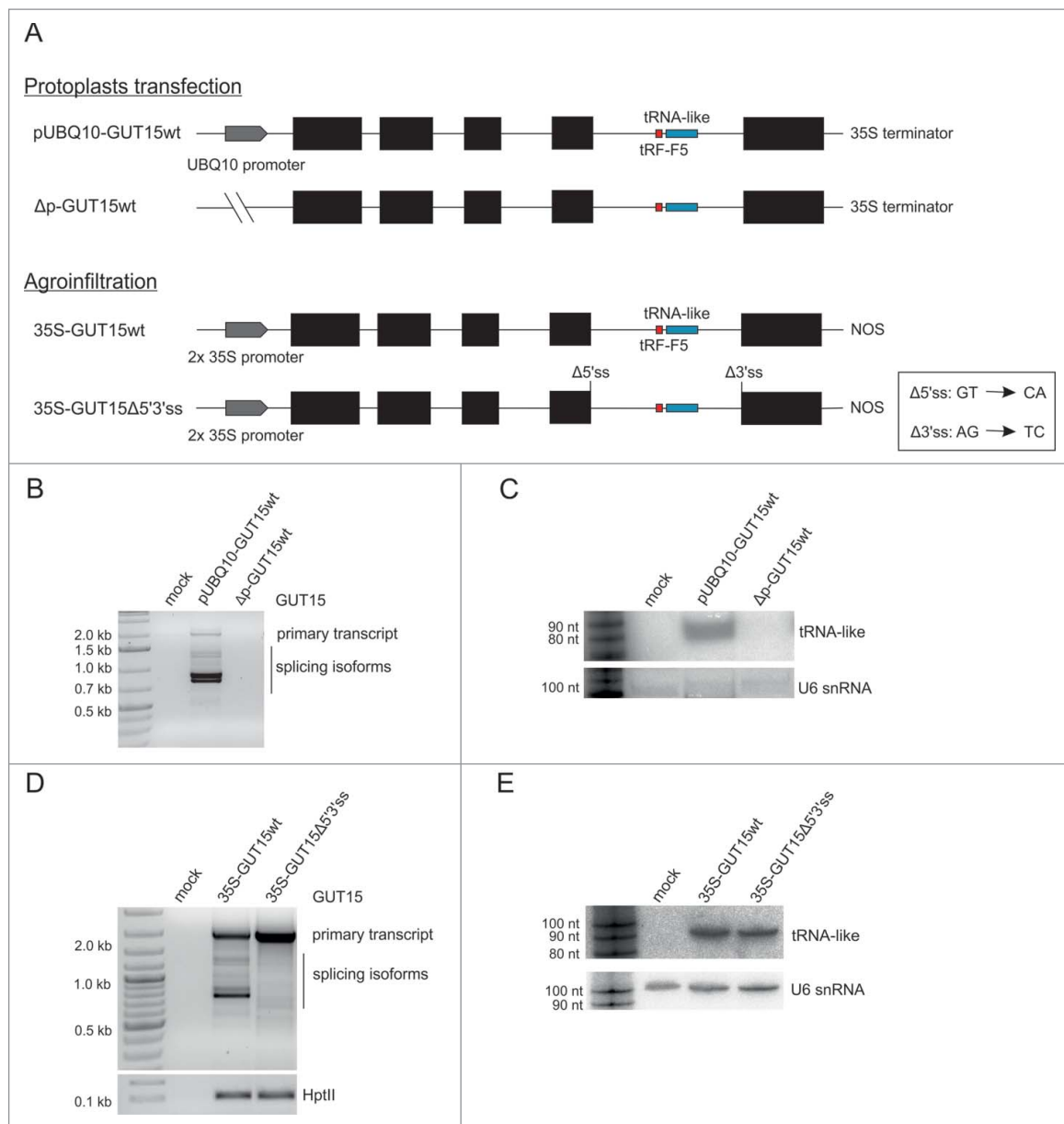


**Figure 3.** The tRNA-like molecule is co-expressed with only the *GUT15* lncRNA. (A) Schematic representation of the *GUT15* gene variants used, and the inactivating 5' ( $\Delta$ 5'ss) and 3' ( $\Delta$ 3'ss) mutations are presented in the box. Black boxes represent exons, and lines depict introns. The splice sites and positions of the tRNA-like and *GUT15*-tRF-F5 sequences are marked in blue and red, respectively. NOS, transcription terminator; UBQ 10, ubiquitin promoter. (B) Primary transcripts and splicing isoforms of *GUT15* recorded by RT-PCR in transfected tobacco protoplasts expressing the *GUT15* gene variants shown in A (upper panel). MOCK is a negative control for the transfection. Marker, 1 kb plus (Thermo Fisher Scientific). (C) The levels of tRNA-like sequence detected by Northern blotting in tobacco protoplasts expressing the *GUT15* variants shown in A (upper panel). U6 snRNA serves as an RNA loading control. Marker, Decade<sup>TM</sup> Marker RNA (Thermo Fisher Scientific). (D) Primary transcripts and splicing isoforms of *GUT15* analyzed by RT-PCR in infiltrated *N. benthamiana* leaves expressing the *GUT15* gene variants shown in A (bottom panel). The expression of the hygromycin phosphotransferase gene (*HptII*) served as a positive control for the agroinfiltration experiment. MOCK is a negative control for the agroinfiltration experiment (leaves infiltrated only with MES buffer). Marker, 100 bp plus (Thermo Fisher Scientific). (E) The levels of the tRNA-like molecule detected by Northern blotting in infiltrated *N. benthamiana* leaves expressing the *GUT15* variants shown in A (bottom panel). U6 snRNA serves as an RNA loading control. Marker, Decade<sup>TM</sup> Marker RNA (Thermo Fisher Scientific).

according to the investigation of the specific copy numbers of the isoforms using an qPCR-based absolute quantification method, the *GUT15* intron lacking the tRNA-like sequence (pGUT15 $\Delta$  construct) was excised more efficiently than the other two intron variants (pGUT15 and pGUT5(Ala)) (Fig. 5C, left panel). These observed changes are consistent with our previous tobacco agroinfiltration experimental results.

To determine whether the tRNA-like molecule and tRNA-Ala<sup>AGC</sup> affect the splicing of intronic sequences, additional constructs were prepared and tested in transfected tobacco

protoplasts. We selected *CBP80* (*CAP-BINDING PROTEIN 80*; At2g13540) intron number 3 (similar in size to the *GUT15* tRNA-like hosting intron) [20], which does not naturally possess any tRNA-resembling elements. The original intron construct was modified to contain either the *GUT15* tRNA-like sequence or tRNA-Ala<sup>AGC</sup> (called pCBP80(tRNA-like) and pCBP80(Ala), respectively) (Fig. 5B, right panel). RT-qPCR analysis confirmed the inhibitory effect of the *GUT15* tRNA-like molecule but not that of tRNA-Ala<sup>AGC</sup> on *CBP80* intron 3 splicing (Fig. 5C, right panel). Therefore, the presence of tRNA

**Table 2.** Protein-coding genes overlapping annotated tRNA genes in the sense orientation in *Arabidopsis* genome.

Gene symbol / annotation	tRNA	Context
AT1G64130 – polyketide cyclase/dehydrase and lipid transport superfamily	LeuCCA	CDS/intron
AT1G68760 – nudix hydrolase 1 hydrolyzes 8-oxo-(d)GTP to 8-oxo-(d)GMP	ProAGG	3'-UTR
AT1G71697 – choline kinase 1 increased in response to wounding	GlyGCC	3'-UTR
AT2G07771 – cytochrome C assembly protein	IleAAU*	CDS/3'-UTR
AT4G24030 – unknown protein	GlyCCC	CDS/3'-UTR
AT2G24390 – AIG2-like (avirulence induced gene) family protein	ArgACG	5'-UTR (longest mRNA isoform)
AT4G03410 – peroxisomal membrane 22 kDa (Mpv17/PMP22) family protein	GlnCUG	5'-UTR
AT4G25640 – detoxifying efflux carrier 35, multidrug and toxin efflux family transporter	LeuCAA	CDS (mRNA isoform 2)
AT5G07630 – lipid transporter	LeuCAA	CDS/intron
AT5G45720 – AAA-type ATPase family protein DNA polymerase III complex	GluUUC	3'-UTR
AT2G07681 – cytochrome C assembly protein	IleAAU*	intron
AT2G07706 – unknown protein	MetCAU*	intron
AT2G07815 – cytochrome C biogenesis	GlyGCC*	intron
AT3G11402 – Cys/His-rich C1 domain family protein	ValCAC	intron
AT3G12587 – oligosaccaryltransferase	ArgCCG	intron
AT4G02060 – minichromosome maintenance (MCM2/3/5) family protein	HisGUG	intron (longest isoform, alternative transcription initiation)
AT2G36145 – unknown protein	AsnGUU	intron
AT5G39530 – unknown function (DUF1997)	ProAGG	intron
AT5G57880 – multipolar spindle 1 involved in meiotic spindle organization	MetCAU	intron

\*potential pseudogenes

loci within introns of RNAPII-dependent genes does not generally interfere with the splicing of their primary transcripts. However, the tRNA-like sequence from the *GUT15* gene inhibits the splicing of the introns in which it is embedded.

## Discussion

The *GUT15* lncRNA was first identified in the tobacco BY-2 cell line as a transcript with a relatively short half-life [15]. In contrast, *GUT15* RNA was found among highly stable transcripts in pollen from *N. tabacum* plants [21]. This differential stability suggests that the regulation of the *GUT15* RNA lifetime is tissue specific [21]. Interestingly, two *Arabidopsis* lncRNAs, the *GUT15* and *CR20-1*, are hormonally regulated members of a family conserved among monocots and dicots [22,23]. Using a 3'-RACE approach, we confirmed that the

*AtGUT15* lncRNA is polyadenylated [23], which is similar to *AtCR20-1* [22]. Furthermore, we demonstrated that *AtGUT15* is capped and undergoes alternative splicing. The same mRNA-like features have also been observed in mammalian and other plant lncRNAs [4, 6, 24].

*AtGUT15* and *AtCR20-1* are known to share a highly similar segment that forms a stable secondary structure [25], and a part of this conserved region is present in another location of the *Arabidopsis* genome (chromosome 1), suggesting that this region could be potentially targeted by the sequence-specific activity of the *GUT15/CR20* gene family [23]. Our computational analysis revealed the presence of a second conserved region within the *Arabidopsis* *GUT15* locus. We identified a tRNA-resembling sequence in its final intron (intron 4). Notably, a highly similar sequence, i.e., lacking twelve nucleotides and differing by

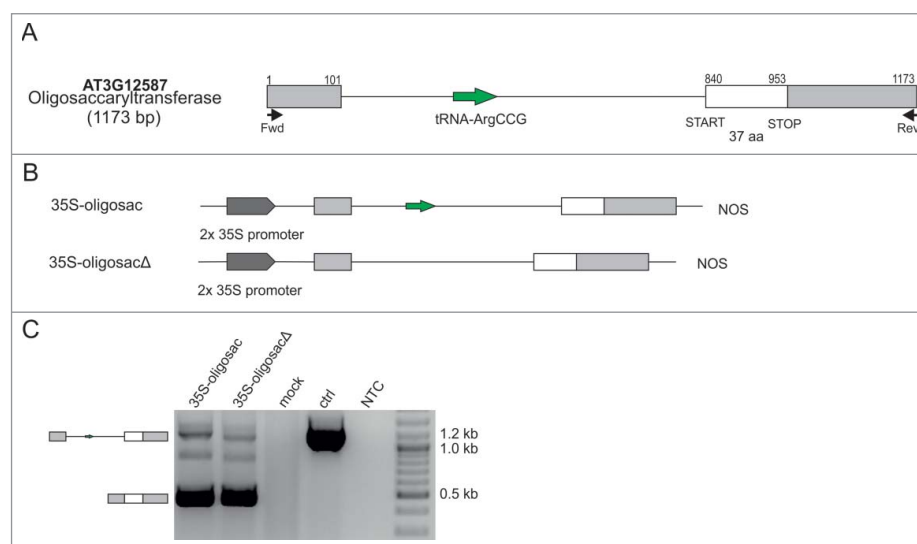


**Figure 4.** Standard tRNAs do not affect the splicing of their hosting genes. (A) Schematic structure of the *At3g12587* hosting tRNA-Arg<sup>CCG</sup> within its intron. The white box represents an exon, the gray boxes represent UTRs, the lines depict introns, and the arrow corresponds to the tRNA (adapted from TAIR10). (B) Schematic representation of the oligosaccaryltransferase gene variants used. NOS, transcription terminator. (C) Splicing isoforms of the oligosaccaryltransferase transcript recorded by RT-PCR in infiltrated *N. benthamiana* leaves expressing the oligosaccaryltransferase gene variants shown in B. Schematic structures of the identified isoforms are presented on the left. MOCK is a negative control for the agroinfiltration experiment (leaves infiltrated only with MES buffer). ctrl, amplification of genomic DNA; NTC, non-template control; and marker, 100 bp plus (Thermo Fisher Scientific).

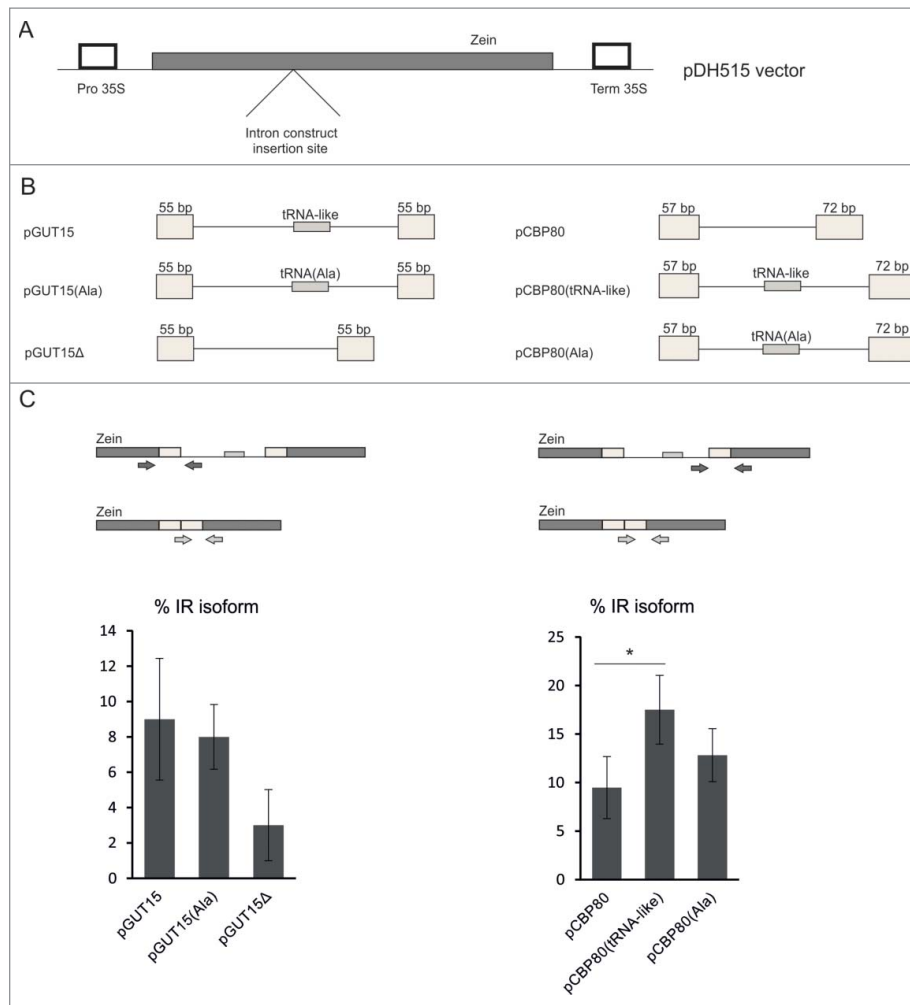


**Figure 5.** Schematic representation of the intron constructs used to examine the splicing of the tRNA/tRNA-like carrying introns. (A) Schematic structure of the pDH515 vector with marked positions of the inserted intron constructs. Closed box, the zein gene; open boxes, the CaMV 35S promoter and terminator regions. (B) Schematic diagrams of the intron constructs used. Boxes represent exons, and lines depict introns. The sizes of the original exon fragments used in the constructs are shown. (C) RT-qPCR analysis of the splicing efficiency of particular intron constructs. Arrows shown in the upper part of the panel with the intron mini-construct schemes depict the primers used. Intron retention isoform levels were calculated as a percentage of all splicing events (intron retained (IR) plus fully spliced (FS) transcripts, treated as 100%) identified within the analyzed intron. Error bars indicate SD ( $n = 3$ ), and the asterisk indicates a significant difference in the splicing efficiency between the native construct and the mutated constructs ( $*p < 0.05$ ).

only a few nucleotides, is also located within the second exon of the *Arabidopsis CR20-1* gene (Fig. S1A). Similar to the *GUT15*-encoded tRNA-like sequence, this sequence does not fold into a secondary structure with canonical anticodon stem-loop characteristics (Fig. S1B); however, this sequence was not identified among actively transcribed tRNAs or tRNA-resembling genes according to our tRNA-seq data. Importantly, the tRNA-like molecule from *AtGUT15* is recognized by the tRNA maturation machinery, as evidenced by its 3'-end CCA motif that is not encoded in the genome. This posttranscriptional modification specific to mature tRNA molecules has recently been shown to be present (a complete or partial CCA-terminus) in certain non-tRNA substrates, such as the *rps12*, *cox2* and *atp9* mitochondrial mRNA transcripts in maize, human spliceosomal U2 snRNA and the 3'-end of the tobacco mosaic virus RNA [26]. The biological consequences of these unusual nucleotide incorporations remain unexplored and may reflect unspecific reactions of CCA-adding enzymes [26] because most of these transcripts contain a stem-loop

structure at the 3'-end that resembles the tRNA minihelix, which is known to be an efficient substrate for CCA-addition *in vitro* [27,28].

In addition to having the CCA sequence, the *GUT15*-encoded tRNA-like molecule was detected only in the tRNA-seq library prepared from the deacylated tRNA fraction, suggesting that this molecule may be charged by an amino acid. The biological role of this newly identified tRNA-like sequence, notably its potential involvement in protein translation, remains to be elucidated. However, certain plant-specific RNA viral genomes contain tRNA-like structures that can be specifically aminoacylated by valine, histidine and tyrosine, and this tRNA mimicry is important for diverse aspects of viral infectivity [29]. In bacteria, it plays a role in tagging abnormal proteins for proteolysis [30].

Furthermore, the tRNA-like molecule from *AtGUT15* is not expressed by RNAPIII and instead is processed from the *GUT15* transcripts synthesized by RNAPII. A similar mechanism has been reported for two tRNA-like molecules generated from the mammalian lncRNAs *MALAT1* and *Menβ*. In both

cases, RNase P recognizes the tRNA-like structure in a nascent RNAPII transcript and cleaves it to simultaneously generate the 3'-end of the mature nuclear-retained lncRNA and the 5'-end of the tRNA-like small RNA [31, 32]. Recently, 132 genomic loci resembling the *MALAT1* 3'-end processing module have been identified among several vertebrate genomes [33]. Interestingly, both mascRNAs (MALAT1-associated small cytoplasmic RNAs) and the *GUT15*-tRNA-like molecule are marked with a CCA [31]. Furthermore, the RNAPII-mediated transcription of conventional tRNAs has been already reported for tRNA<sup>Sec</sup> in *Trypanosoma brucei* [34].

The *AtGUT15* transcript serves as a precursor for another small noncoding RNA, the *GUT15*-tRF-F5. This small RNA is also generated from the final intron of the *AtGUT15* lncRNA. Interestingly, the *GUT15* tRNA-like sequence exerts an inhibitory effect on both the splicing of its host intron and *GUT15*-tRF-F5 biogenesis. Therefore, the *GUT15*-tRF-F5 fragment may be produced from the spliced intron. In contrast, the accumulation of *GUT15* tRNA-like molecules is not influenced by *GUT15* lncRNA splicing, suggesting that it is not produced from the intron excised from the *AtGUT15* primary transcripts.

The *GUT15* lncRNA has been previously characterized as a peptide-coding transcript, because both *N. tabacum* and *A. thaliana* genes contain putative short open reading frames (sORFs) of 78 and 75 amino acids, respectively [16]. In 2016, an sORF encoding a 37-aa peptide was identified in *GUT15* in *Arabidopsis* roots using the Ribo-Seq method [35]. However, this peptide does not correspond to the 75-aa peptide predicted by van Hoof and coworkers [40]. This peptide has homologs in multiple species within the *Brassicaceae* family [35], but the function of this conserved short peptide is unknown. In the same study, additional 26 small ORFs were identified in annotated lncRNAs. These are not the only cases of transcripts believed to solely function as RNA molecules that do in fact code for small peptides [12,36]. In our studies we also detected the *AtGUT15* transcripts to be attached to translating ribosomes. Interestingly, only the isoform lacking the tRNA-like sequence was associated with polyribosomal fractions (Fig. S2). Thus, we speculate that the spliced version of the *GUT15* transcript can physically interact with ribosomes to produce a small peptide from its first exon, whereas primary *GUT15* transcripts serve as a source of tRNA-like molecules. In contrast, Carlevaro-Fita et al. [37] have recently shown that ribosomes are the default destination of most cytoplasmic lncRNAs and may play a role in their degradation because blocking ribosomal elongation results in the stabilization of many associated lncRNAs, which may be also the case for the *GUT15* lncRNA. In 1995, Taylor and coworkers found that the level of the shorter *GUT15* transcript was significantly increased in an actinomycin D (inhibitor of RNAPII transcription)- and cycloheximide (translational inhibitor)-treated tobacco cell line [15]. Therefore, a complex regulatory mechanism underlies the biogenesis and functions of the noncoding RNAs and small peptides originating from the *GUT15* lncRNA.

Our experiments shed light on the phenomena of tRNA and tRNA-like sequences embedded within introns of their host genes. By screening the TAIR10 database, we identified 19 host protein-coding genes containing annotated tRNAs in their

introns and UTRs in a sense orientation. Additionally, our global approach revealed two *Arabidopsis* lncRNAs, *GUT15* and *CR20-1*, that contain similar tRNA-like sequences in their intron and exon, respectively. Our transient expression experiments in tobacco protoplasts confirmed the negative effects of the *GUT15* tRNA-like sequence on the splicing of both its original host and the *CBP80* intron. Similarly, this influence was also observed when the tRNA-Ala<sup>AGC</sup> gene was inserted into the *AtGUT15* intron, suggesting that this effect may be due to this specific intron. Moreover, the tRNA-Arg<sup>CCG</sup> embedded in the oligosaccharyltransferase gene does not affect the splicing pattern of its transcript. Accordingly, we conclude that the presence of a tRNA coding sequence in the host protein-coding genes does not interfere with gene splicing. Interestingly, Zhang and coworkers [38] revealed an additional role of tRNA sequences in systemic mRNA transport in plants. These authors found that mobile mRNAs in *Arabidopsis* are enriched in tRNA-like motifs or are transcribed from genes located in close proximity to annotated tRNA loci, which form di-cis-tronic mRNA-tRNA transcripts at a high frequency (according to paired-end RNA-seq data). However, the *GUT15* lncRNA was not identified among the genes producing mobile transcripts [39], suggesting that the tRNA-related sequence derived from this lncRNA plays other roles.

## Materials and methods

### Plant material and growth conditions

*Arabidopsis thaliana* Columbia-0 wild-type plants were grown for 10 or 14 days as previously described [40].

*N. benthamiana* and *N. tabacum* var. Xanthi plants were grown for 4 and 8 weeks, respectively, at 22°C (16/8-hour light/dark cycle, 50% humidity, and 150–200  $\mu\text{mol m}^{-2} \text{s}^{-1}$  photon flux density).

### Construct preparation

For the agroinfiltration of the tobacco leaves, the genomic sequences of At2g18440 (*GUT15*) and At3g12587 (gene encoding oligosaccharyltransferase) were amplified (from *A. thaliana* genomic DNA isolated using the DNeasy Plant Mini Kit, Qiagen) and cloned into the pCR8 plasmid (Thermo Fisher Scientific) using the *NotI* and *AscI* restriction sites. The *GUT15* and oligosaccharyltransferase constructs lacking the tRNA-like or tRNA sequences were created using a three-step PCR approach as previously described [40]. The mutagenesis of the *GUT15* final intron splice sites was performed using the QuikChange II Site-Directed Mutagenesis Kit (Agilent Technologies). To detect the expression in plants, the At2g18440 and At3g12587 gene versions were cloned into the pMDC32 Gateway binary vector [41] using the Gateway LR Clonase II Enzyme Mix (Thermo Fisher Scientific).

For transient expression in the tobacco protoplasts, Gateway LR Clonase II Enzyme Mix was used to generate expression clones carrying the genomic sequence of At2g18440 without or under the control of the UBQ10 promoter.

The intron mini-constructs were based on the following two *Arabidopsis thaliana* introns: the 4th intron from



*GUT15* (674 bp) and the 3rd intron from the *CBP80* gene (485 bp). The intron sequences together with the fragments (>55 bp) from the original 5'- and 3'-exons were isolated from *Arabidopsis* genomic DNA by PCR and introduced to the plant expression vector pDH515 within an intronless *zein* gene using the unique *Bam*HI restriction site [42,43]. For the mutant intron construct generation (with different tRNA types), a two-step PCR-based approach was used. First, the desired tRNA sequence was amplified from genomic DNA using primers containing intron-specific (*CBP80* or *GUT15*) overhangs. Second, the PCR products were used as primers in the mutagenesis reaction using the appropriate original intron construct as a template and Pfu Ultra High Fidelity polymerase (Agilent Technologies). The sequences of all constructs were verified by Sanger sequencing. All oligonucleotide sequences are listed in Table 3.

### Transient expression in *N. benthamiana* leaves

The tobacco leaf agroinfiltration was performed as previously described [40,44].

### Mesophyll protoplast transfection

The constructs were transfected into protoplasts of *Nicotiana tabacum* var Xanthi isolated from 8-week-old leaves using a previously described protocol for *Arabidopsis* protoplasts with the following modifications [40]: (1) 10  $\mu$ g of the vector were used for the transfection, and (2) the transfected protoplasts were incubated overnight in the dark at 22°C before RNA isolation using a modified TRIzol method [45].

### RNA isolation and cDNA preparation

For the Northern blot, RACE, qPCR and RT-PCR analyses, total RNA from 100 mg of tissue or protoplast suspensions was isolated using the TRIzol reagent (Thermo Fisher Scientific) or the Direct-zol<sup>TM</sup> RNA MiniPrep Kit (ZymoResearch). For the small RNA library construction and stem-loop reverse transcription, total RNA enriched for small RNAs was isolated from 100 mg of 14-day-old *A. thaliana* seedlings using a previously described protocol [46]. The integrity and quality of the NGS-dedicated RNA were verified using an Agilent RNA 6000 Nano Kit (Agilent Technologies).

For the cDNA preparation, total RNA was first treated with Turbo DNase I (Thermo Fisher Scientific); double treatment was required for RNA isolated from transfected protoplasts. The reverse transcription reactions were prepared from 0.5–3  $\mu$ g of total DNase-treated RNA using SuperScript III Reverse Transcriptase (Thermo Fisher Scientific) and either the oligo-dT<sub>(18)</sub> primer (Thermo Fisher Scientific) or the *Zein*-specific primer. The stem-loop pulsed reverse transcription was performed using 200 ng of total RNA enriched for small RNAs [47].

### sRNA-seq, tRNA-seq and bioinformatics analyses

*A. thaliana* total RNA enriched for the small RNA species was used for the small RNA library generation (TruSeq Small RNA

Library Prep Kit), and sequencing was performed using an Illumina HiSeq 2000 system. A bioinformatics analysis of the sRNA-seq data was performed as previously described [19].

For the tRNA sequencing, total RNA was isolated and deacylated as previously described [48]. After size fractionation in a PAA gel, the RNA molecules (65–100 nucleotides) were used for the library generation, followed by sequencing using an Illumina HiSeq Platform (Fasteris SA, Switzerland). The *GUT15*-encoded tRNA-like molecule was identified from the NGS data by mapping the obtained reads to the *A. thaliana* genome.

The sequence profiles of the A-box and B-box promoter elements were derived by analyzing all *A. thaliana* tRNA genes. The sequence logos in the profiles were produced using the WebLogo application using multiple sequence alignments of corresponding regions from tRNA genes [49].

### Northern blot analyses

For the Northern blot analyses, 5–30  $\mu$ g of total RNA were used to detect sRNA and tRNA-like sequences. The RNA electrophoresis, blot transfer and hybridization were performed as previously described [46,50]. All hybridizations were performed with three biological replicates.

### RT-PCR analyses and quantitative real-time PCR (qPCR)

The RT-PCR amplifications were performed as previously described [51] using the gene-specific oligonucleotide primer pairs listed in Table 3. The amplification of the *GUT15*-encoded tRNA-like molecule was carried out as previously described [47]. The identity of the PCR product was verified by sequencing.

RT-qPCR was performed as previously described [40]. The amplification efficiency of each primer pair was calculated by making a 10-fold dilution series of the plasmid templates, calculating a linear regression based on the data points and estimating the efficiency from the line slope. The primer pairs with the highest almost equal amplification efficiency (max. difference of 10% was approved) and only one visible peak on the dissociation curve were used for the analysis (Table 3).

The expression levels of particular splicing isoforms were calculated by performing the absolute quantification method using standard curves obtained for a 10-fold dilution series of the plasmid bearing the appropriate isoform. To estimate the splicing efficiency, events identified for the analyzed intron (expressed in copy numbers) were summed and treated as 100%, and the contribution of the fully spliced and unspliced isoforms was then calculated.

All results were analyzed using the SDS 2.3 software (Thermo Fisher Scientific). Error bars were calculated using the SD Function in the Microsoft Excel software. The statistical significance of the presented results was estimated using Student's *t*-test at a significance level of \* $p < 0.05$ .

### 3'-, 5'-RACE and 5' RLM-RACE experiments

The 5'- and 3'-RACE cDNA template synthesis and two-step RACE-PCR experiments were conducted using the

Table 3. Oligonucleotides used in this study.

Primers used for constructs preparation			
Name	Sequence	gene/cDNA fragment amplified using the primer pair	Construct prepared using the amplified fragment
A01	ATTGGGGCGGATCACCGCTCCATATCTTTTC	<i>GUT15</i> (At2g18440)	pUBQ10-GUT15wt, Δp-GUT15wt, 35S-GUT15wt, 35S-GUT15Δ, 35S-GUT15Δ5'3' ss
A02	TTTGGCGCCAAITTAATCGTTCAACTATATTTCTATATCTATAAATG	1-1680 bp fragment of <i>GUT15</i>	35S-GUT15Δ
A03	ATCACCGCTCCATATCTTTTC		
A04	ATTTTAAAAATGACGAATAACATATCAGAAATACCTACCACCTACG	1762–2261 bp fragment of <i>GUT15</i>	
A05	TGTTAGGTATTCGTGATGATGTTATGTCATTTTAAAAAATAACTAAGTTATTC	mutagenesis of 5' ss in 35S-GUT15wt	35S-GUT15Δ5'3' ss
A06	AATTAATCGTTCAACTATATTTCTATATCTATAAATG	mutagenesis of 3' ss in 35S-GUT15wt	
A07	CCACAAGATCTTTTGATCAAGATGCTTCAAGAAACAATCAACTTCAGA	<i>Oligosaccaryltransferase</i> (At3g12587)	35S-oligosacΔ
A08	TCTGAAGTTGATTTGTTCTTGAAGCAATCTTGATCAAAAAGATCTGTTGG	1-369 bp fragment of <i>Oligosaccaryltransferase</i>	35S-oligosacΔ
A09	GAGTTCAGTGTGGACAATCGAGTTGATCACAAGAGCAATA	443-1173 bp fragment of <i>Oligosaccaryltransferase</i>	
A10	TATTGCTTTGTGATCAACTCGATGTGCCACACTGAATC	<i>GUT15</i> intron with fragments of flanking exons	pGUT15, pGUT15(Ala), pGUT15Δ
A11	ATTTGGCGCCCTGAGAGTGAGATCCAACTACTTGTCTGT	At1g06610 (tRNA-AlaAGC) with <i>GUT15</i> intron overhangs	pGUT15(Ala)
A12	TTTGGCGCCCAAGAAAAAATTCAAAGTTTCATCAAAACAT	CBP80 (At2g13540) 3rd intron with flanking exons	pCBP80, pCBP80(tRNA-like), pCBP80(Ala)
A13	AAAGACCAAAAAATGGAACTTGGAGAACAAGTGGAAATTTATG	At1g06610 (tRNA-AlaAGC) with <i>CBP80</i> intron overhangs	pCBP80(Ala)
A14	ATTTGGCGCCCTGAGAGTGAGATCCAACTACTTGTCTGT	tRNA-like with <i>CBP80</i> intron overhangs	pCBP80(tRNA-like)
A15	TTTGGCGCCCAAGAAAAAATTCAAAGTTTCATCAAAACAT		
A16	TTTGGCGCCCAAGAAAAAATTCAAAGTTTCATCAAAACAT		
A17	CGGGATCTGAACTATGCAAAAGCTGACGT		
A18	CGGGATCCACACTAGTCAGTTAAGCAAAATAGTACATC		
A19	AGTGTAGGGTATTCGTGATATGAGATGGGATGTAGCTCAGATGGTAG		
A20	AGTTATTTTTAAAAATGACGAATAAATCGGAGATCGGGGTATCGAT		
A21	CGGGATCTTCTTACTACAATGTGCTGAACAATTTG		
A22	CGGGATCCCTGGAAATAGCGTGGACCTTTC		
A23	GTGCTATTATATATATAAATGATGGGATGTAGCTCAGATGGTAG		
A24	AATACATGAATAAATAGATTCCTACATGGAGATCGGGGTATCGAT		
A25	GTGCTATTATATATATAAATGATGGGATGTAGCTCAGATGGTAG		
A26	AATACATGAATAAATAGATTCCTACAGAACTGGGTGGATTGCAACCA		
Primers used in RACE, RT-PCR and qPCR analyses			
Name	Sequence	gene/cDNA fragment amplified using the primer pair	Experiments in which the primer pair was used
B01	TTCGAACCCACCAACCTCTGTCAC	<i>GUT15</i> (At2g18440)	5' RLM-RACE
B02	TCTAGTGGACGAGAGGTGGTGGITCG	<i>GUT15</i> (At2g18440)	3' RACE
B03	ATCACCGCTCCATATCTTTTC	<i>GUT15</i> (At2g18440)	RT-PCR (RACE confirmation)
B04	GGTGAATGATATATATAAGAGTAACAGTACGAT		
B05	TTTGGTCTCCCTCTTTTC	<i>GUT15</i> (At2g18440)	RT-PCR (splicing isoforms analysis)
B06	ACAATCCGCAATTCAAAAGC	<i>Oligosaccaryltransferase</i> (At3g12587)	RT-PCR
B07	CTGAGAGTGAGATCCAATCTGTTCTGT		
B08	AAAAGAAAAAATTCAAAAGTTTCATCAAAACAT	<i>GUT15</i> IR isoform amplification	qPCR
B09	TCCACAACAGCCACAATAA	<i>GUT15</i> FS isoform amplification	qPCR
B10	CCAAATGTTCAACCCTAC	<i>CBP80</i> IR isoform amplification	qPCR
B11	TTTGTCTTGAAGGATGTCC	<i>CBP80</i> FS isoform amplification	qPCR
B12	GGTAAGATGCCTGTGGCATTCG		
B13	TGGAAGTTGATGGATGCTTTTC		
B14	GGTAAGATGCCTGTGGCATTCG		
B15	TTTGTATGGGACTTTGATGGTT		
B16	GGTAAGATGCCTGTGGCATTCG		
B17	ATTTGGCTCCACAATGTC	HptII	RT-PCR
B18	GATGTGGCACCTGAT	Actin2	RT-PCR
B19	GGTAACATTGTGCTCAGTGGTGG		

(Continue on next page)

B20	CTGGCCTTGGAGATCCACATC		
B21	GGAAGAAATTGCTGGGGTA	Zein	Reverse transcription (Zein_RT)
B22	ACCGACAGTAGGAAATGG	At2g36145	RT-PCR
B23	CCTCATGTGACCCCAACT		
B24	TGTGACTATTTGTGCCATGGG	At5g57880	RT-PCR
B25	CCAGTGACTCGGTCCATGTA		
B26	TCCAGATAAGCCCAAGTCA	At5g39530	RT-PCR
B27	TCTAAAGGTACATCTGGCGGA		

## Oligonucleotides used as probes in Northern blot hybridization

Name	Sequence	Detection
C01	GACTCTTAACTATTTT	<i>GUT1</i> 5-rF-F5
C02	ACCAACTCTCGTCCACTAGAAGA	<i>GUT1</i> 5-rRNA-like
C03	TCATCTTGGCAGGGCCA	U6 snRNA

## Oligonucleotides used in stem-loop end-point RT-PCR analysis

Name	Sequence	Experiments in which the primers were used
D01	GTCGTATCCAGTCCAGGGTCCGAGGTATTCGCACTGGATACGACTGGCAG	stem-loop reverse transcription primer
D02	TGGTAGAGCGCTCGTTTCT	end-point RT-PCR of rRNA-like from <i>GUT1</i> 5
D03	GTGCAGGGTCCGAGGT	

SMARTer RACE cDNA Amplification Kit (Clontech) according to the manufacturer's protocol. The cDNA template used in the 5'-RLM-RACE analysis was created using the GeneRacer™ Kit (Thermo Fisher Scientific) according to the manufacturer's protocol. PCR reactions were performed using the Advantage 2 PCR Enzyme System (Clontech) on a Veriti thermal cycler (Applied Biosystems). PCR products were cloned into the pGEM T-Easy vector (Promega) and sequenced. The primer sequences are listed in Table 3.

## Disclosure of potential conflicts of interest

No potential conflicts of interest were disclosed.


## Acknowledgments

The authors would like to thank Dr. Katarzyna D. Raczynska and Dr. Kamilla Bakowska-Zywicka for their help with the polysome profiling and Dr. Andrzej Pacak and Dr. Maria Barciszewska-Pacak for their help with the small RNA library construction.

## Funding

This work was supported by the National Science Center under grant numbers UMO-2013/11/N/NZ2/02511 (awarded to PP), UMO-2013/10/A/NZ1/00557 (awarded to AJ) and UMO-2011/03/B/NZ2/01416 (awarded to WMK); the Foundation for Polish Science under grants Mistrz 3.5/2014 (awarded to AJ) and START 32.2017 (awarded to KK); and the KNOW RNA Research Center in Poznan (01/KNOW2/2014).

## ORCID

Agnieszka Thompson  <http://orcid.org/0000-0003-0566-006X>

## References

- [1] Kung JTY, Colognori D, Lee JT. Long noncoding RNAs: Past, present, and future. *Genetics*. 2013;193(3):651–669. doi:10.1534/genetics.112.146704
- [2] Engreitz JM, Ollikainen N, Guttman M. Long non-coding RNAs: spatial amplifiers that control nuclear structure and gene expression. *Nat Rev Mol Cell Biol*. 2016;17(12):756–770. doi:10.1038/nrm.2016.126
- [3] Liu X, Hao L, Li D, et al. Long Non-coding RNAs and Their Biological Roles in Plants. *Genomics Proteomics Bioinformatics*. 2015;13(3):137–147. doi:10.1016/j.gpb.2015.02.003
- [4] Swiezewski S, Liu F, Magusin A, et al. Cold-induced silencing by long antisense transcripts of an Arabidopsis Polycomb target. *Nature*. 2009;462(7274):799–802. doi:10.1038/nature08618
- [5] Heo JB, Sung S. Vernalization-Mediated Epigenetic Silencing by a Long Intronic Noncoding RNA. *Science* (80-). 2011;331(6013):76–79. doi:10.1126/science.1197349
- [6] Ariel F, Jegu T, Latrasse D, et al. Noncoding Transcription by Alternative RNA Polymerases Dynamically Regulates an Auxin-Driven Chromatin Loop. *Mol Cell*. 2014;55(3):383–396. doi:10.1016/j.molcel.2014.06.011
- [7] Ben Amor B, Wirth S, Merchan F, et al. Novel long non-protein coding RNAs involved in Arabidopsis differentiation and stress responses. *Genome Res*. 2009;19(1):57–69. doi:10.1101/gr.080275.108
- [8] Wierzbicki AT, Haag JR, Pikaard CS. Noncoding Transcription by RNA Polymerase Pol IVb/Pol V Mediates Transcriptional Silencing of Overlapping and Adjacent Genes. *Cell*. 2008;135(4):635–648. doi:10.1016/j.cell.2008.09.035
- [9] Franco-Zorrilla JM, Valli A, Todesco M, et al. Target mimicry provides a new mechanism for regulation of microRNA activity. *Nat Genet*. 2007;39(8):1033–1037. doi:10.1038/ng2079
- [10] Wang Y, Fan X, Lin F, et al. Arabidopsis noncoding RNA mediates control of photomorphogenesis by red light. *Proc Natl Acad Sci*. 2014;111(28):10359–10364. doi:10.1073/pnas.1409457111
- [11] Ding J, Lu Q, Ouyang Y, et al. A long noncoding RNA regulates photoperiod-sensitive male sterility, an essential component of hybrid rice. *Proc Natl Acad Sci U S A*. 2012;109(7):2654–2659. doi:10.1073/pnas.1121374109
- [12] Campalans A, Kondorosi A, Crespi M. Enod40, a Short Open Reading Frame-Containing mRNA, Induces Cytoplasmic Localization of a Nuclear RNA Binding Protein in *Medicago truncatula*. *Plant Cell*. 2004;16(4):1047–1059. doi:10.1105/tpc.019406
- [13] Bardou F, Ariel F, Simpson CG, et al. Long Noncoding RNA Modulates Alternative Splicing Regulators in Arabidopsis. *Dev Cell*. 2014;30(2):166–176. doi:10.1016/j.devcel.2014.06.017
- [14] Seo JS, Sun H-X, Park BS, et al. ELF18-INDUCED LONG-NONCODING RNA Associates with Mediator to Enhance Expression of Innate Immune Response Genes in Arabidopsis. *Plant Cell*. 2017;29(5):1024–1038. doi:10.1105/tpc.16.00886
- [15] Taylor CB, Green PJ. Identification and characterization of genes with unstable transcripts (GUTs) in tobacco. *Plant Mol Biol*. 1995;28(1):27–38.
- [16] Ambro van Hoof, James P, Kastenmayer CBT and PJG. GUT15 cDNAs from Tobacco (Accession No. U84972) and Arabidopsis (Accession No. U84973) Correspond to Transcripts with Unusual Metabolism and a Short Conserved ORF. *Plant Physiol*. 1997;113:1004.
- [17] Söll D, RajBhandary U. *TRNA: Structure, Biosynthesis, and Function*. ASM Press; 1995.
- [18] Lamesch P, Berardini TZ, Li D, et al. The Arabidopsis Information Resource (TAIR): improved gene annotation and new tools. *Nucleic Acids Res*. 2012;40(Database issue):D1202–10. doi:10.1093/nar/gkr1090
- [19] Thompson A, Zielezinski A, Plewka P, et al. tRex: A Web Portal for Exploration of tRNA-Derived Fragments in Arabidopsis thaliana. *Plant Cell Physiol*. 2018;59(1):e1–e1. doi:10.1093/pcp/pcx173
- [20] Kmiecik M, Simpson CG, Lewandowska D, et al. Cloning and characterization of two subunits of Arabidopsis thaliana nuclear cap-binding complex. *Gene*. 2002;283(1):171–183. doi:10.1016/S0378-1119(01)00859-9
- [21] Ylstra B, McCormick S. Analysis of mRNA stabilities during pollen development and in BY2 cells. *Plant J*. 1999;20(1):101–108. doi:10.1046/j.1365-313X.1999.00580.x
- [22] Teramoto H, Toyama T, Takeba G, et al. Noncoding RNA for CR20, a cytokinin-repressed gene of cucumber. *Plant Mol Biol*. 1996;32(5):797–808. doi:doi.org/10.1007/BF00020478
- [23] MacIntosh GC, Wilkerson C, Green PJ. Identification and Analysis of Arabidopsis Expressed Sequence Tags Characteristic of Non-Coding RNAs. *Plant Physiol*. 2001;127(November):765–776. doi:10.1104/pp.010501.cient
- [24] Liu J, Jung C, Xu J, et al. Genome-Wide Analysis Uncovers Regulation of Long Intergenic Noncoding RNAs in Arabidopsis. *Plant Cell*. 2012;24(11):4333–4345. doi:10.1105/tpc.112.102855
- [25] Cheng Lu, Gustavo MacIntosh PG. Two Non-coding RNAs, AtGUT15 and AtCR20, modulate the ABA response at high temperature in Arabidopsis. 501707136
- [26] Vörtler S, Mörl M. tRNA-nucleotidyltransferases: Highly unusual RNA polymerases with vital functions. *FEBS Lett*. 2010;584(2):297–302. doi:10.1016/j.febslet.2009.10.078
- [27] Shi PY, Weiner AM, Maizels N. A top-half tDNA minihelix is a good substrate for the eubacterial CCA-adding enzyme. *RNA*. 1998;4(3):276–284.
- [28] Li Z, Sun Y, Thurlow DL. RNA minihelices as model substrates for ATP/CTP:tRNA nucleotidyltransferase. *Biochem J*. 1997;327(Pt 3):847–851.
- [29] Dreher TW. Role of tRNA-like structures in controlling plant virus replication. *Virus Res*. 2009;139(2):217–229. doi:10.1016/j.virusres.2008.06.010



- [30] Keiler KC, Waller PRH, Sauer RT. Role of a Peptide Tagging System in Degradation of Proteins Synthesized from Damaged Messenger RNA. *Science* (80- ). 1996;271(5251):990–993. doi:10.1126/science.271.5251.990
- [31] Wilusz JE, Freier SM, Spector DL. 3' end processing of a long nuclear-retained noncoding RNA yields a tRNA-like cytoplasmic RNA. *Cell* .2008;135(5):919–932. doi:10.1016/j.cell.2008.10.012
- [32] Sunwoo H, Dinger ME, Wilusz JE, et al. MEN epsilon/beta nuclear-retained non-coding RNAs are up-regulated upon muscle differentiation and are essential components of paraspeckles. *Genome Res*. 2009;19(3):347–359. doi:10.1101/gr.087775.108
- [33] Zhang B, Mao YS, Diermeier SD, et al. Identification and Characterization of a Class of MALAT1-like Genomic Loci. *Cell Rep*. 2017;19(8):1723–1738. doi:10.1016/j.celrep.2017.05.006
- [34] Aeby E, Ullu E, Yepiskoposyan H, et al. tRNA<sup>Sec</sup> is transcribed by RNA polymerase II in *Trypanosoma brucei* but not in humans. *Nucleic Acids Res*. 2010;38(17):5833–5843. doi:10.1093/nar/gkq345
- [35] Hsu PY, Calviello L, Wu H-YL, et al. Super-resolution ribosome profiling reveals unannotated translation events in *Arabidopsis*. *Proc Natl Acad Sci*. 2016;113(45):E7126–E7135. doi:10.1073/pnas.1614788113
- [36] Rohrig H, Schmidt J, Miklashevichs E, et al. Soybean ENOD40 encodes two peptides that bind to sucrose synthase. *Proc Natl Acad Sci U S A*. 2002;99(4):1915–1920. doi:10.1073/pnas.022664799
- [37] Carlevaro-Fita J, Rahim A, Guigó R, et al. Cytoplasmic long noncoding RNAs are frequently bound to and degraded at ribosomes in human cells. *RNA* .2016;22(6):867–882. doi:10.1261/rna.053561.115
- [38] Zhang W, Thieme CJ, Kollwig G, et al. tRNA-Related Sequences Trigger Systemic mRNA Transport in Plants. *Plant Cell*. 2016;28(6):1237–1249. doi:10.1105/tpc.15.01056
- [39] Thieme CJ, Rojas-Triana M, Stecyk E, et al. Endogenous *Arabidopsis* messenger RNAs transported to distant tissues. *Nat Plants*. 2015;1(4):15025. doi:10.1038/nplants.2015.25
- [40] Knop K, Stepien A, Barciszewska-Pacak M, et al. Active 5' splice sites regulate the biogenesis efficiency of *Arabidopsis* microRNAs derived from intron-containing genes. *Nucleic Acids Res*. 2016;323(5):gkw895. doi:10.1093/nar/gkw895
- [41] Curtis MD, Grossniklaus U. A gateway cloning vector set for high-throughput functional analysis of genes in planta. *Plant Physiol*. 2003;133(2):462–469. doi:10.1104/pp.103.027979
- [42] Simpson CG, Clark G, Davidson D, et al. Mutation of putative branchpoint consensus sequences in plant introns reduces splicing efficiency. *Plant J*. 1996;9(3):369–380. doi:10.1046/j.1365-313X.1996.09030369.x
- [43] Lewandowska D, Simpson CG, Clark GP, et al. Determinants of plant U12-dependent intron splicing efficiency. *Plant Cell*. 2004;16(5):1340–1352. doi:10.1105/tpc.020743
- [44] Bielewicz D, Kalak M, Kalyna M, et al. Introns of plant pri-miRNAs enhance miRNA biogenesis. *EMBO Rep*. 2013;14(7):622–628. doi:10.1038/embor.2013.62
- [45] Chomczynski P, Sacchi N. The single-step method of RNA isolation by acid guanidinium thiocyanate-phenol-chloroform extraction: twenty-something years on. *Nat Protoc*. 2006;1(2):581–585. doi:10.1038/nprot.2006.83
- [46] Kruszka K, Pacak A, Swida-Barteczka A, et al. Developmentally regulated expression and complex processing of barley pri-microRNAs. *BMC Genomics*. 2013;14(1):34. doi:10.1186/1471-2164-14-34
- [47] Varkonyi-Gasic E, Wu R, Wood M, et al. Protocol: a highly sensitive RT-PCR method for detection and quantification of microRNAs. *Plant Methods*. 2007;3:12. doi:10.1186/1746-4811-3-12
- [48] Gaston KW, Rubio MAT, Alfonzo JD. OXOPAP assay: For selective amplification of aminoacylated tRNAs from total cellular fractions. *Methods*. 2008;44(2):170–175. doi:10.1016/j.ymeth.2007.10.003
- [49] Crooks G, Hon G, Chandonia J, et al. NCBI GenBank FTP Site\nWebLogo: a sequence logo generator. *Genome Res*. 2004;14:1188–1190. doi:10.1101/gr.849004.1
- [50] Pall GS, Hamilton AJ. Improved northern blot method for enhanced detection of small RNA. *Nat Protoc*. 2008;3(6):1077–1084. doi:10.1038/nprot.2008.67
- [51] Raczynska KD, Ruepp M-D, Brzek A, et al. FUS/TLS contributes to replication-dependent histone gene expression by interaction with U7 snRNPs and histone-specific transcription factors. *Nucleic Acids Res*. 2015;43(20):9711–9728. doi:10.1093/nar/gkv794